

Locating good conductors by using the B-field integrated from partial dB/dt waveforms of time-domain EM systems

Haoping Huang, Geo-EM, LLC

Summary

An approach for computing the B-field from time-domain dB/dt data measured by an induction coil has been developed. When the dB/dt samples do not cover the whole waveform, the constant of integration can be readily determined from the scheme without any assumptions. Theoretical modeling and tests on airborne time-domain electromagnetic data show that the B-field response integrated from the dB/dt data considerably enhances responses to good conductors and suppresses responses of overburden, making identification and interpretation of good conductors easier. This process can be accomplished either in an EM receiver in real time or from dB/dt data that were already acquired.

Introduction

Time-domain electromagnetic (EM) systems have been increasingly used in mineral exploration. The targets of interest are generally good conductors with slow decays with time. Currently, most time-domain EM systems use an induction coil to measure the time derivatives (dB/dt) of the secondary magnetic fields (B-field). The responses to good conductors will come from slowly decaying, low-amplitude magnetic fields and those to overburden from rapidly decaying, high amplitude fields. The B-field has significantly greater energy at low frequencies, while the dB/dt contains more energy at high frequencies. Having more energy at low frequencies is advantageous for detecting conductive targets as indicated by many authors (e. g., Sarma et al., 1976; McCracken et al., 1986; Eaton and Hohmann, 1987; Smith and Annan, 1998; Wolfgram and Thomson, 1998). Therefore, considerable efforts have been made to obtain the B-field response from either an induction coil indirectly or a magnetometer directly (Lamontagne, 1975; West et al., 1984; Foley and Leslie, 1998; Smith and Annan, 1998; Wolfgram and Thomson, 1998 and Smith and Annan, 2000). Smith and Annan (1998, 2000) and Wolfgram and Thomson (1998) present the B-field responses integrated from airborne time-domain EM dB/dt data measured using an induction coil sensor. Some experiments using a SQUID magnetometer as the sensor in ground and airborne transient EM surveys are reported by Duckworth and O'Neill (1989), Foley and Leslie (1998), Foley et al (1999), Osmond et al. (2002) and Annison (2004).

Computing the B-field from the dB/dt data by the integration requires measuring the whole waveform. If the

dB/dt samples do not cover the whole waveform, a constant of integration should be determined. Otherwise, a dc shift in the integrated B-field response occurs. Levy (1984) described a technique for integrating the B-field response from dB/dt data. However, the constant of integration can not be determined because the sensor used to acquire the data is incapable of measuring the whole waveform. Since many time-domain EM systems are incapable of measuring the whole waveform, some approaches for determining the constant of integration have been attempted. An algorithm described by Eaton and Hohmann (1987) iteratively determines the dc shift by assuming a power law or an exponential for the late-time decay. Another approach that may eliminate the dc shift is to deconvolve dB/dt data to step response (Holladay, 1981; Wolfgram and Karlik, 1995 and Stolz and Macnae, 1997). As indicated by Smith and Annan (2000), this can be an unstable process because the spectrum of the transmitter waveform does not have information at certain frequencies, and this introduces noise into the process. An approximate deconvolution method described by Eaton (1998) has been demonstrated to work well for converting airborne EM data to the step response.

Recently, a scheme has been developed to derive the B-field response from partial dB/dt data. The constant of integration can be numerically determined. The intention of this paper is to present some results from theoretical modeling and tests on real data.

Theoretical modeling

For time-domain EM systems that are capable to acquire the full waveform information in digital form, the B-field response can be obtained by integrating the dB/dt data from an induction coil sensor (Smith and Annan, 2000). For EM systems without this capability, it is also possible to compute the B-field response from the dB/dt data and determine the constant of integration using a digital integration technique.

Let's consider a bipolar triangle waveform of transmitting current as shown in Figure 1a, where τ is the width of the current pulse and T the period. The primary voltage measured by an induction coil is shown in Figure 1b. The power spectra on Figure 1c show difference between the two waveforms. The dB/dt spectrum peaks around the fifth harmonic, and falls off slowly as frequency increasing. There is more energy at high frequencies. The B-field has greater energy at the first and third harmonics and the response falls off rapidly with frequency, resulting less energy at high frequencies. Therefore, the B-field measurements enhance the responses of good conductors,

Locating good conductors by using the B-field

and suppress responses of relatively resistive materials, for example, overburden.

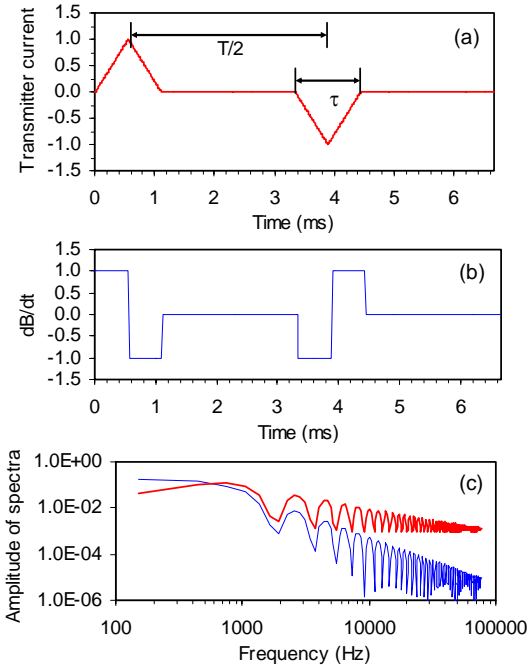


Figure 1: (a) A transmitter current waveform. There is a triangle pulse 1.1 ms wide, followed by an off time of 2.2 ms and then a second half cycle of opposite polarity. (b) The normalized waveform as measured by an induction coil (dB/dt). (c) The power spectra of the dB/dt (red) and B-field (blue) primary waveforms.

First, it is assumed that data sampling covers the whole waveform. For an illustration of the results, the dB/dt response of a 10-S horizontal thin sheet has been computed. The transmitting coil is a small horizontal loop at 50 m above the sheet and the receiving coil is a vertical dipole at the center of the transmitter. Figure 2 depicts the dB/dt and B-field responses. There are two B-field response curves, one is computed theoretically (in red) and the other obtained by the integration of the dB/dt data (in blue). Both curves are virtually identical, except for the computation errors attributed to the finite precision of the numerical integration.

Then, let's examine the case of the partial data samples. Figure 3a illustrates an example, where the dB/dt data are only available within the windows as shown in this figure. The theoretical B-field curve (in red) in Figure 2b is replotted for comparison. The integrated B-field response from the partial dB/dt data is shown in green. As we have seen, both on-time and off-time B-field responses shift up

by a constant in the first half period. Once the constant is determined from the scheme, the B-field can be corrected as shown by the blue curve in Figure 3a.

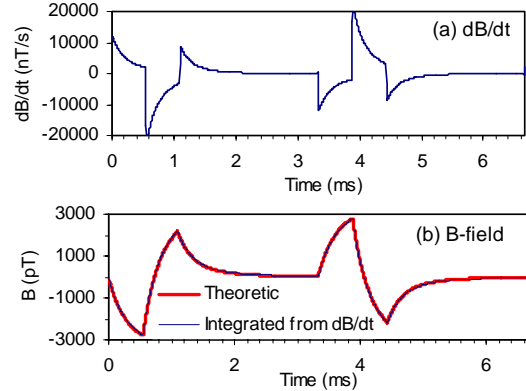


Figure 2: (a) The dB/dt response to a 10-S infinite horizontal thin sheet at 50 m below the transmitting loop. (b) The B-field data computed theoretically (red) and integrated (blue) from the dB/dt data.

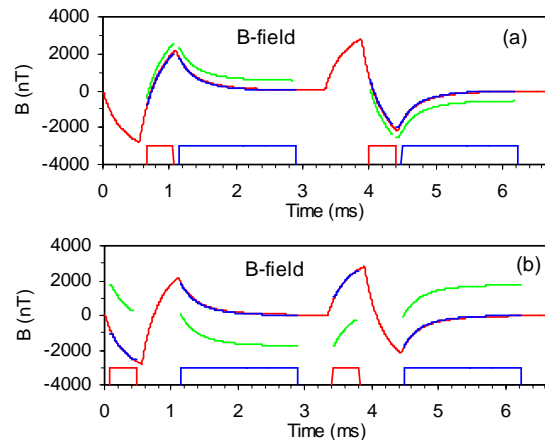


Figure 3: Theoretic B-field response (in red) replotted from Figure 2b and integrated B-field responses (in green and blue) from the dB/dt data that do not cover the whole waveform. The boxes at the bottom of the panels indicate the sampling windows, the red ones for on time and the blue for off time. The curves in green show the dc shift and those in blue are the dc shift corrected. (a) The on-time window is from 0.65 to 1 ms and (b) from 0.15 to 0.45 ms.

The dc shift depends upon the dB/dt sample distribution over the waveform, as well as the properties of target. Figure 3b shows the results from the same model as that in Figure 3a, but the on-time sampling window is moved to the first half pulse. As we have noted, the dc shift is much larger than that in Figure 3a. Also, the shift goes up in the

Locating good conductors by using the B-field

on-time window and down in the off-time window in the first half period, and the shift is larger for the on-time data than for the off-time data. After the dc shifts are corrected, the B-field response (in blue) matches the theoretical solution.

Field example

The technique has been tested on a variety of real datasets and some results from these tests will be shown below.

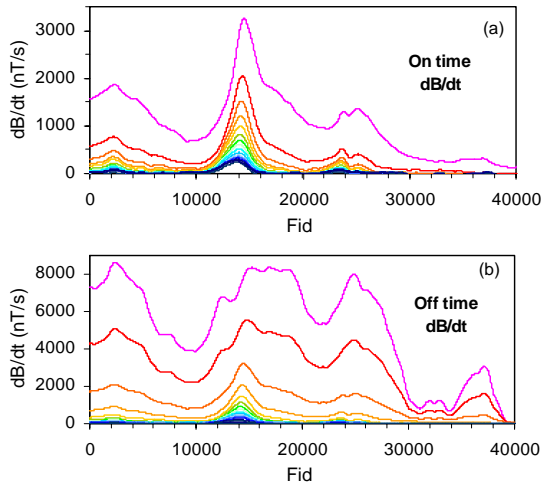


Figure 4: The vertical components of the on-time (a) and off-time (b) dB/dt data measured using an AeroTEM system operating at 150-Hz base frequency. The warm color stands for the earlier time channel and the cool color for the later.

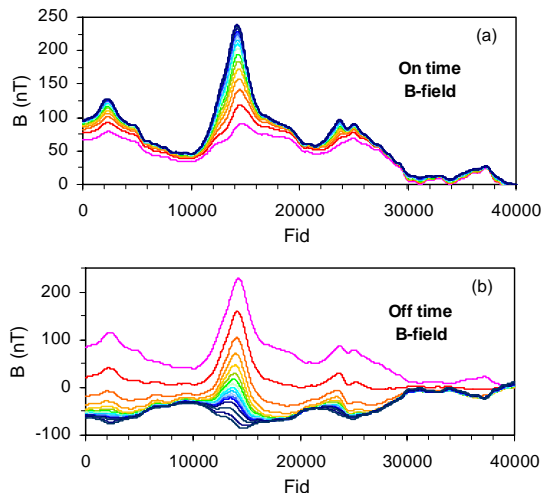


Figure 5: The B-field data derived from the dB/dt data shown on Figure 4, but without correcting the dc shifts. (a) On time and (b) off time.

The data for the first example were collected using a time-domain helicopter-borne EM system (AeroTEM) operating at 150-Hz base frequency (Huang and Rudd, 2006). The transmitting waveform is a bipolar triangular pulse as shown in Figure 1a. The vertical and horizontal components of the dB/dt data are measured using induction coils during the transmitter on time and off time. However, the on-time data are sampled only for the half transmitter on time. Figure 4 shows the vertical components of the on-time and off-time dB/dt data from a flight line. From the on-time dB/dt data, we see a distinctive anomaly at 14,000, and two small anomalies at 2,200 and 23,500. The large anomaly is clearly seen on the off-time dB/dt profile, but the others are hardly identified. Also, large responses on the early off-time channels seem to be caused by the near surface materials.

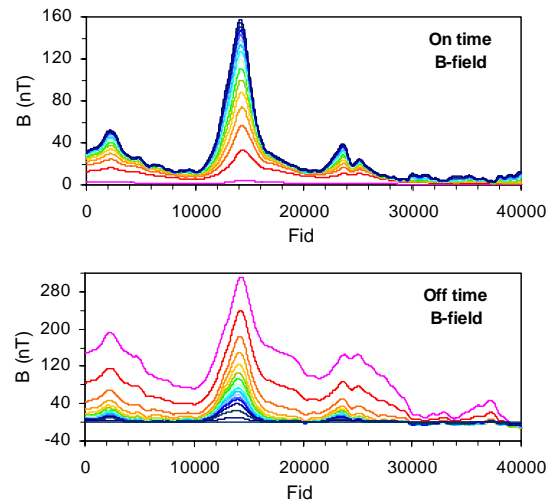


Figure 6: The B-field data after the dc shift correction. (a) On time and (b) off time.

Figure 5 is the B-field data derived from the dB/dt data in Figure 4. The dc shifts are not corrected. The three anomalies become more evident, especially on the off-time profile. Because of the dc shifts, the two anomalies at 2,200 and 14,000 are distorted on the late off-time channels. It is obvious that this problem cannot be fixed by any filtering or leveling techniques since the dc shifts vary from data point to data point. The dc shifts are simultaneously determined during the process and can be subtracted from the integrated B-field responses. Figure 6 shows the B-field data after the dc corrections. Comparing the B-field responses with the dB/dt data in Figure 4, the three anomalies are significantly enhanced on both on-time and off-time profiles and the large responses of the near surface materials are drastically suppressed.

Locating good conductors by using the B-field

Figure 7 illustrates profiles of on-time and off-time dB/dt and B-field responses from another AeroTEM survey. As we can see, it is much easier to locate, discriminate and interpret the anomalies from the B-field responses than from the dB/dt data.

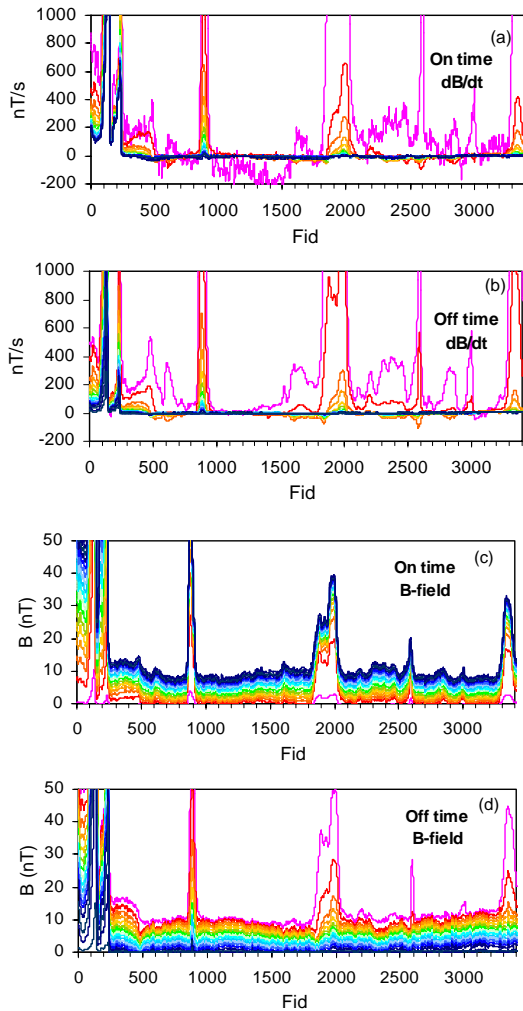


Figure 7: The on-time (a) and off-time (b) dB/dt responses. The on-time (c) and off-time (d) B-field responses integrated from the dB/dt data.

Figure 8 demonstrates maps of the dB/dt and B-field responses from a mid-channel at off time. Comparing the two maps, we see that the small, confined anomalies, i.e., A, B and C, are enhanced on the B-field map, in particular for C which can be seen clearly in two flight lines on the B-field map, but only in one flight line on the dB/dt map. Anomaly D is better located on the B-field map. Also, the

feature (E) caused by relatively resistive materials becomes weaker on the B-field map.

Conclusions

An approach for computing the B-field from the dB/dt data measured by an induction coil has been developed. When the dB/dt data do not cover the full waveform, the constant of integration can be readily determined from the scheme, which does not require making any assumptions. This process can be done either in an EM receiver in real time or from the dB/dt data that were already acquired. As shown in the examples, the B-field response integrated from the dB/dt data considerably enhances the responses to good conductors and suppresses the response of the near surface materials. This makes identification and interpretation of good conductors easier. In practice, using B or dB/dt depends upon the purpose of a survey. If the target is good conductors, such as massive sulphide deposits, the B-field response will be definitely superior to the dB/dt data. However, the dB/dt response will be better than the B-field if surveys are for geological mapping, determining depth to bedrock, groundwater exploration, etc., where the targets are resistive.

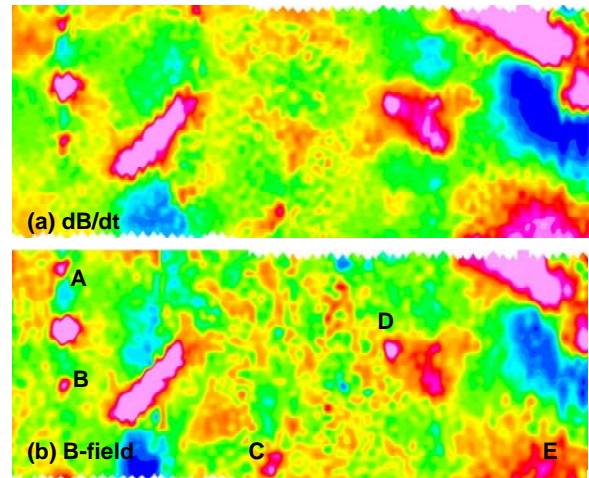


Figure 8: Maps of the dB/dt data (a) and the B-field (b) response derived from the dB/dt data.

EDITED REFERENCES

Note: This reference list is a copy-edited version of the reference list submitted by the author. Reference lists for the 2007 SEG Technical Program Expanded Abstracts have been copy edited so that references provided with the online metadata for each paper will achieve a high degree of linking to cited sources that appear on the Web.

REFERENCES

- Annisson, C., 2004, B-Field TEM data acquisition for nickel exploration: Preview, 111, 96.
- Duckworth, K., and D. O'Neill, 1989, Detection of a brine conductor under an oil field by means of a fixed transmitter electromagnetic survey using a squid magnetometer: Canadian Journal of Exploration Geophysics, 25, 61–73.
- Eaton, P. A., 1998, Application of an improved technique for interpreting transient electromagnetic data: Exploration Geophysics, 29, 175–183.
- Eaton, P. A., and G. W. Hohmann, 1987, An evaluation of electromagnetic methods in the presence of geologic noise: Geophysics, 52, 1106–1126.
- Foley, C. P., and K. E. Leslie, 1998, Potential use of high Tc SQUIDS for airborne electromagnetics: Exploration Geophysics, 29, 30–34.
- Foley, C. P., K. E. Leslie, R. Binks, C. Lewis, W. Murray, G. J. Sloggett, S. Lam, B. Sankrithyan, N. Sawides, A. Katzaros, K.-H. Muller, E. E. Mitchell, J. Pollock, J. Lee, D. L. Dart, R. R. Barrow, M. A. Asten, A. Maddever, G. Panjkovic, M. Downey, C. Hoffman, and R. Turner, 1999, Field trials using HTS SQUID magnetometers for ground-based and airborne geophysical applications: IEEE Transactions of Applied Superconductivity, 9, 3786–3792.
- Holladay, J. S., 1981, YVESFT and CHANNEL, A subroutine package for stable transformation of sparse frequency domain data to the time domain: Research in Applied Geophysics, 17.
- Huang, H., and J. Rudd, 2006, Conductivity-depth imaging of time-domain AEM data based on pseudo-layer half-space model: 76th Annual International Meeting, SEG, Expanded Abstracts, 765–769.
- Lamontagne, Y., 1975, Applications of wideband, time-domain EM measurements in mineral exploration: Ph.D. thesis, University of Toronto.
- Levy, G. M., 1984, Correction of measured transient electromagnetic responses for finite transmitter turn-off duration: Geonics Technical Note TN-16.
- McCracken, K. G., M. L. Oristaglio, and G. W. Hohmann, 1986, A comparison of electromagnetic exploration systems: Geophysics, 51, 810–818.
- Osmond, R., A. W. Watts, W. R. Ravenhurst, C. Foley, and K. Leslie, 2002, Finding nickel from the B-field at Raglan - 'To B or not dB': 72nd Annual International Meeting, SEG, Expanded Abstracts, 404–407.
- Sarma, D. G., V. M. Maru, and G. Varadarajan, 1976, An improved pulse transient airborne electromagnetic system for locating good conductors: Geophysics, 41, 287–299.
- Smith, R. S., and A. P. Annan, 1998, The use of B-field measurements in an airborne time-domain system — Part I: A comparison of B-field with dB/dt measurements: Exploration Geophysics, 29, 24–29.
- , 2000, Using an induction coil sensor to indirectly measure the B-field response in the bandwidth of the transient electromagnetic method: Geophysics, 65, 1489–1494.
- Stolz, E. M., and J. C. Macnae, 1997, Fast approximate inversion of TEM data: Exploration Geophysics, 28, 317–322.
- West, G. F., J. C. Macnae, and Y. Lamontagne, 1984, A time-domain EM system measuring the step response of the ground: Geophysics, 49, 1010–1026.
- Wolfgang, P., and G. Karlik, 1995, Conductivity-depth transform of GEOTEM data: Exploration Geophysics, 26, 179–185.
- Wolfgang, P., and S. Thomson, 1998, The use of B-field measurements in an airborne time-domain system — Part II: Examples in conductive regimes: Exploration Geophysics, 29, 225–229.